Evaluation of Amplified Image Characteristics of a BSO Crystal

Raphael A. Guerrero, Darwin Z. Palima, and Marlon Rosendo H. Daza*
National Institute of Physics
College of Science, University of the Philippines
Diliman, Quezon City 1101
E-mail: mdaza@nip.upd.edu.ph

ABSTRACT

Image amplification by two-wave missing in a BSO crystal is investigated. Amplified images are observed to have higher gray levels, with an average relative gain of 5.9. Contrast range is enhanced from 0-to-58 to 0-to-98 and the overall brightness is increased by a factor of 2.7. The response function of the image amplification system shows sensitivity at higher spatial frequencies and is similar for two different images.

INTRODUCTION

Current computer technology is still primarily electronics-based. A way of overcoming the limitations of electronic technology is by using several computers in parallel. Parallel optical processors represent the next level of computer technology with their inherent ability to process two-dimensional arrays of data at extremely high speeds (Kawata et al., 1990a). Recently, photorefractive crystals (PRCs) have been recognized as promising components in the manufacture of optical-parallel active elements (Joseph et al., 1995). The ability of PRCs to record dynamic volume holograms makes possible the real-time implementation of various processing and computing operations. Logical AND and OR operations have already been performed with $BaTiO_3$, a diffusion-type crystal (Joseph et al., 1995). In terms of potential for real-time processing, BSO is a prime candidate among these PRCs due to its fast grating-writing time (Kawata et al., 1990b).

Two-wave mixing (TWM) in a PRC makes possible the coherent amplification of images in parallel without performing optical-to-electronic conversion. Image amplification is achieved on a strictly optical-to-optical basis. A coherent image amplifier not only provides gain to an input signal but also maintains fidelity between the input and output signals. Such a device is essential for optical operational amplifiers, optical feedback systems and logical memory (Joseph et al., 1995).

Previous work in this field focused mainly on the dynamics of the amplification process in PRCs. Unfortunately, the literature available on photorefractive image amplification lacks a discussion on the actual quality of the amplified image. Hence, this paper is an initial attempt to design, implement, and characterize a coherent image amplifier using a photorefractive crystal. The results are intended to complement the present database regarding the potential of PRCs in optical computing.

The discussion of this work will take the following form. Basic photorefractive theory and the fundamentals of image amplification are presented in section II. The experimental set-up, as well as the procedures used,

Key words: nonlinear optics, image processing

**Corresponding author*

are discussed in section III. Section IV summarizes the results. Finally, section V gives the conclusions obtained from this work.

IMAGE AMPLIFICATION THEORY

Image amplification is an application of two-wave mixing (Fig. 1), a process made possible by the photorefractive effect which occurs in several types of nonlinear crystals and liquid crystals. The photorefractive effect was discovered in 1966, when it was still referred to as "optical damage" (Yeh, 1992).

The *photorefractive effect* is a bulk phenomenon in which the local index of refraction of the material is modulated by illumination of light with spatially varying intensity (Yeh, 1992). Examples of photorefractive crystals are $LiNbO_3$, $BaTiO_3$ and BSO. The spatially varying intensity can be generated by interfering two laser beams within the crystal. This results in the formation of bright and dark fringes. Due to the resulting photoionization in the bright region, charge carriers drift and diffuse to the dark regions, where they are trapped. The eventual charge separation and the periodic intensity within the photorefractive crystal lead to a space charge field. This field, in return, induces a change in the index of refraction via the linear electro-optic (Pockels') effect.

Once a photorefractive effect has been established inside the crystal, two coherent beams of light undergo energy coupling where there is a non-reciprocal energy transfer between the two. This process is known as *two wave mixing* (Yeh, 1993). The photorefractive effect produces a volume index grating within the material. Since the Bragg scatterings are perfectly phase-matched, the two incident light waves are strongly diffracted. One beam is diffracted in the direction of the other beam and vice versa.

In certain crystals such as BSO, energy coupling only becomes optimal with a moving interference pattern and an applied external electric field (E_0). A method of generating moving fringes is by using a mirror attached to a piezoelectric transducer (PZT). Fringes formed due to the interference move with a velocity given by:

$$\hat{v} = 2 f_{pzt} d \tag{1}$$

Here, f_{pzt} and d are the PZT's frequency and maximum displacement, respectively. The movement of the fringes in the direction of the applied voltage complements the index grating shift introduced by E_0 so that there is energy coupling between the beams.

Usually, one beam (the signal) has a lower intensity

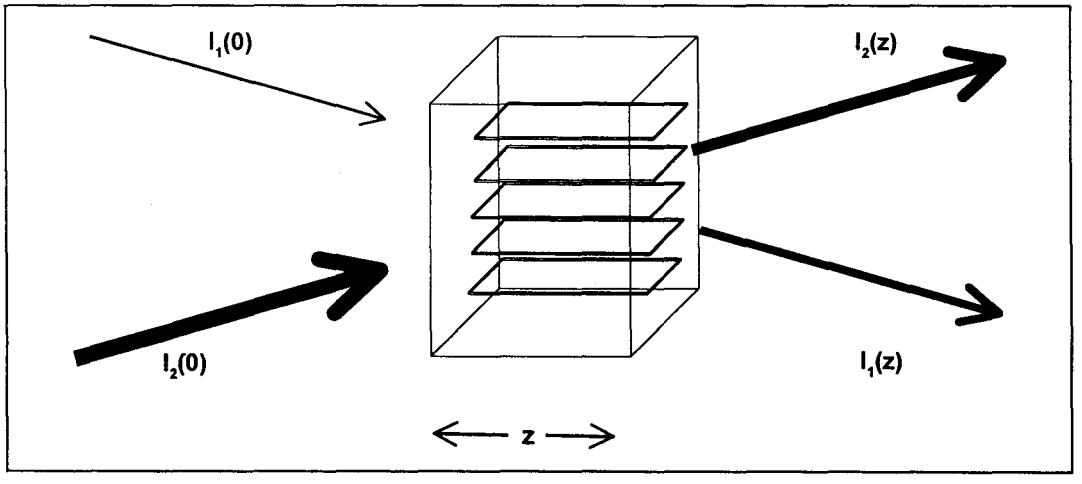

Fig. 1. Two-wave mixing in a PRC

than the other beam (the pump). The energy coupling in TWM transfers energy from the stronger pump beam to the weaker signal beam (Yeh, 1993). The signal beam's intensity increases at the expense of the pump beam. The linear gain, Γ, for a signal beam passing through the crystal is given by Tarroja-Keller et al. (1997)

$$\Gamma = \frac{1+m}{1+m\exp(-\gamma z_0)}. \quad (2)$$

Here, $m = I_{pump}/I_{signal}$ is the ratio between the intensities of the pump and signal beams, γ is the gain coefficient and z_0 is the length of the crystal. The gain coefficient, γ, is a function of θ, the angle between the beams (Tarroja-Keller et al., 1997). θ is also related to the grating wavelength. For BSO, the angle between the beams is usually small. In TWM, Γ is maximum at one value of θ for particular values of applied external field and fringe velocity. For the TWM experiments in this study, Γ was the definition of the gain used.

An application of the energy transfer in two-wave mixing is image amplification. For an image-bearing wave consisting of many plane wave components, the gain of the image-bearing beam, I_d, can be expressed as:

$$\frac{I_d(z)}{I_d(0)} = \frac{1+m}{1+m\exp(-\Gamma z)} \quad (3)$$

where z is the crystal length and

$$m = \frac{I_p(0)}{\sum_{d=1}^{N} I_d(0)} \quad (4)$$

I_p is the pump beam intensity. Except for the definition of m in Equation 4, the gain is similar to that in TWM.

EXPERIMENTAL SET-UP

The experimental set-up is shown in Fig. 2. Image amplification experiments are performed with a 1 cm x 1 cm x 1 cm BSO crystal. The coherent light source is a 514 nm air-cooled Ar^+ laser (Omnichrome 543–AP–A01). Beam expansion and collimation are performed with 2 lenses of focal lengths 3 cm (L1) and 15 cm (L2). The beam is split into a pump beam and a signal beam. The signal beam is attenuated with a series of neutral density (ND) filters, passed through an image mask and a Melles-Griot resolution target, and focused into the crystal with a 50 cm lens. A voltage (V_0) ranging from 1-6 kV is applied across the crystal. The pump beam is phase-shifted by a mirror attached to a piezo-electric transducer (Melles-Griot) with a PZT driver controlled by a signal generator. The pump beam is then made to interfere with the signal beam inside the crystal. The output is recorded with a Hamamatsu C3077 CCD camera.

The target is placed 100 cm from the lens, with a similar distance for the CCD camera. This distance is twice the focal length of the lens, leading to a magnification factor of 1and producing a sharp image at the plane of the CCD. The camera is interfaced to a DIPIX P360f Power Grabber to collect the images. The original and amplified 8-bit gray-scale images obtained from the CCD camera have default frame grabber dimensions of 512 pixels wide by 474 pixels high. The Fourier transforms provided by the frame grabber are 256 x 256.

Upon initial calibration of the set-up, a maximum gain of 2.7 ± 0.4 is achieved for θ = 1.8° and an applied voltage of 6 kV. The PZT frequency (f) is 0.11 Hz and m is 9.63.

Two sets of image amplification experiments are performed. The first set determines the amplification per pixel of an image. Gain for this experiment is set at 2.3 ± 4. Eight frames of an image with gain and without gain are grabbed and converted into RAW format. One line of pixels is chosen arbitrarily (line 290) and a C program is used to extract the pixel gray levels. Extracted gray levels are assigned values from 0 to 255. The average gray value per pixel for 8 frames is plotted. Noise levels are minimized by the averaging process as well as the absence of extraneous light sources. The pixel intensity values of the amplified images are then compared to those of the original, unamplified images. A histogram for the entire image is obtained by tabulating all gray levels present in both unamplified and amplified images.

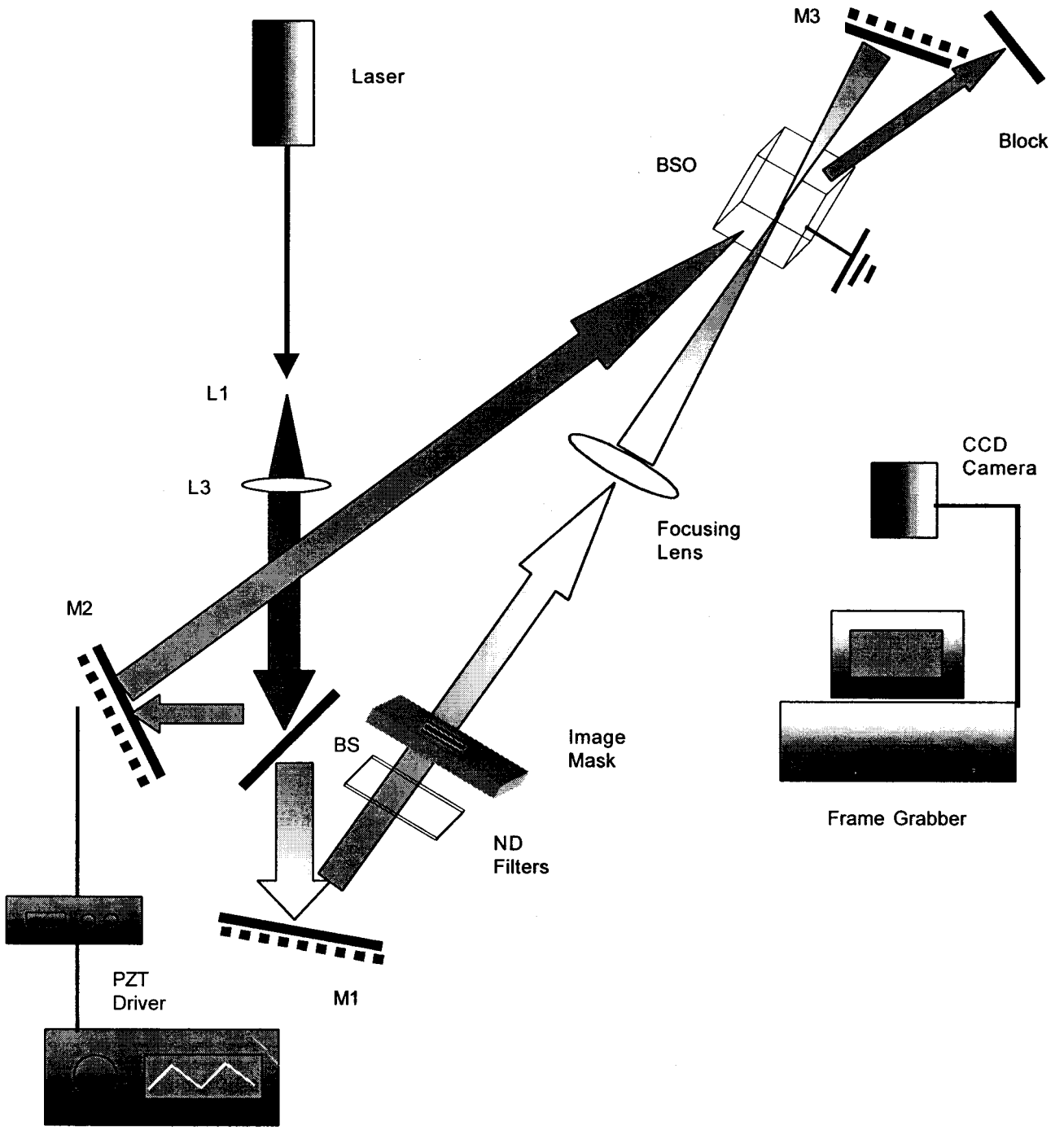

Fig. 2. Image amplification set-up

The second experiment is performed to determine the response function of the system and to establish the fidelity of image information upon amplification. During one run with gain = 2.7, two different sections of the resolution target (see inset in Fig. 2), designated as Images A (the topmost square) and B (the circle at the lower right), are amplified. The Fourier transforms of the amplified and unamplified images are then calculated. In extracting gray levels, only the central x-axes of the 2D Fourier transforms are used. The FT of the response function is obtained by dividing the amplified image FT by the FT of the unamplified image.

RESULTS AND DISCUSSION

Fig. 3 shows the unamplified (3a) and amplified (3b) images obtained from the experiment.

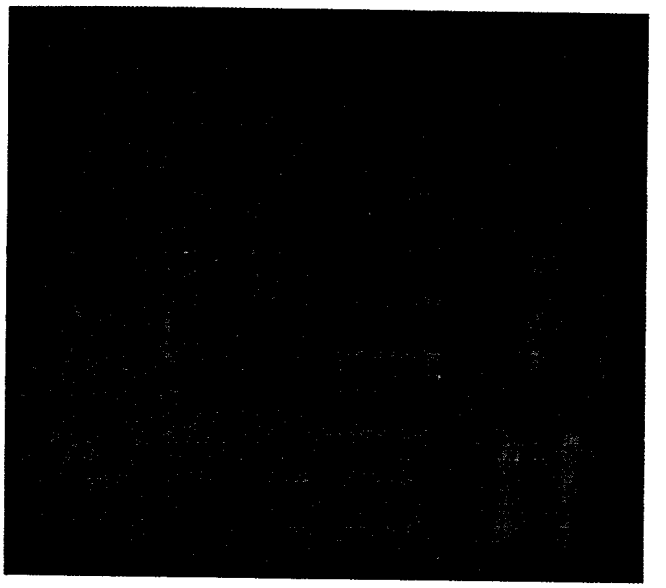

Fig. 3a. Image without amplification

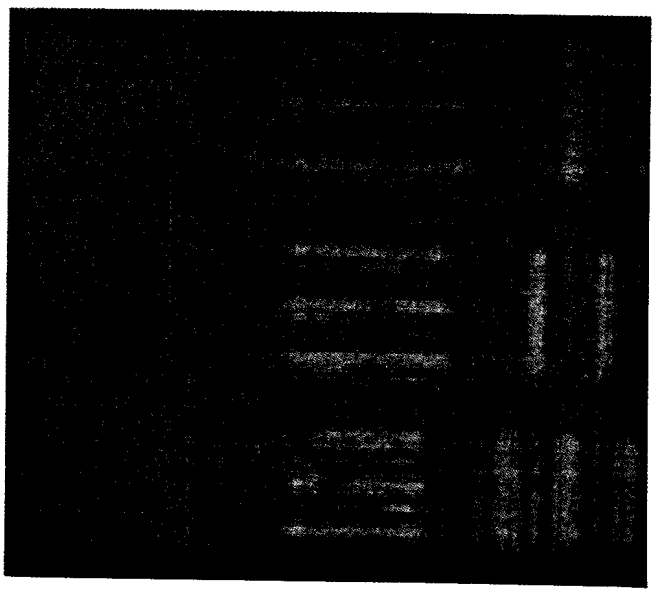

Fig. 3b. Image with amplification

Although it is possible to show all 474 lines, a single line conveniently shows the intensity increase. Fig. 4 summarizes the increase in the intensity of the pixels for Line 290. The maximum gray level rises from 36 to 91 and the average gray level from 8 to 28. The average relative gain has a value of 5.9. The results indicate a significant increase in pixel intensity for this particular line scan. Also, the line scan shows that intensity levels in the non-illuminated areas remain approximately constant. Essentially, the bright regions become brighter and the dark regions remain dark, leading to a higher image visibility.

The histogram for the amplified image is given in Fig. 5a. Comparing this with the unamplified histogram (Fig. 5b), it can be seen that a wider range of pixel gray values are present. Whereas the unamplified image has gray values from 0 to 58, the amplified image's gray values range from 0 to 98. This wider range of gray values implies improved contrast in the image. The integrated optical density (IOD), the weighted sum of the histogram, of the amplified image has a value of 2738047 compared to the original IOD of 1008369. This result means an increase in the overall brightness of the image. The gain in IOD (2.7) falls within the experimental value of TWM gain. The IOD and histogram mainly imply that the image has been enhanced in terms of contrast and overall intensity.

Image A (Fig. 6a) and Image B (Fig. 6b) are used to determine the response function of the photorefractive amplifier. Assuming an amplification which takes the form of a convolution $g = h * f$, where g and f are the amplified and original image functions, respectively, the Fourier transforms of these images should determine the response function h.

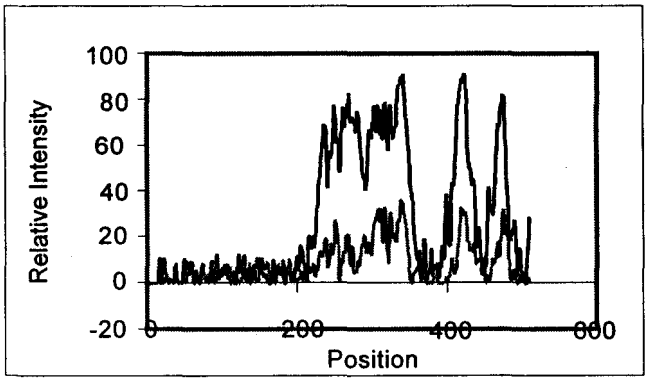

Fig. 4. Intensity scan of Line 290 comparing unamplified (gray) and amplified (black) gray levels.

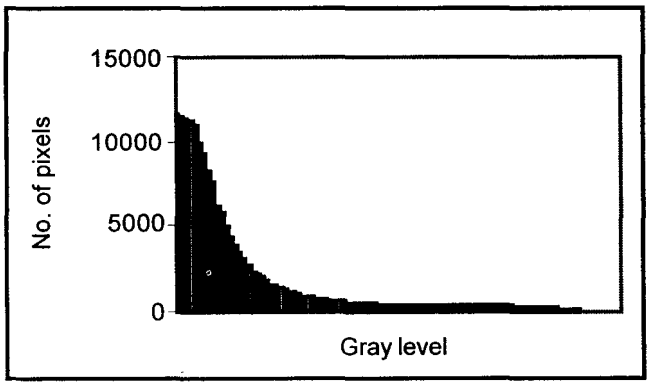

Fig. 5a. Histogram of amplified image.

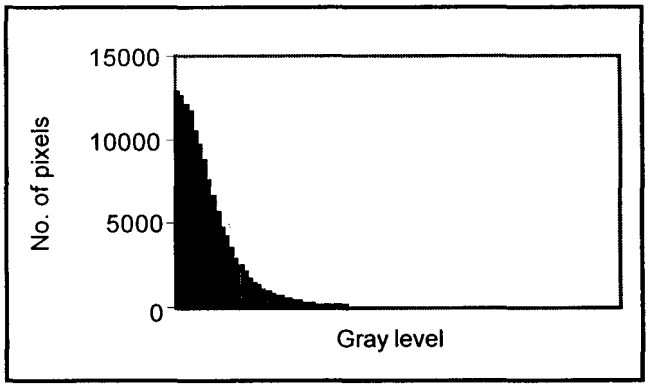

Fig 5b: Histogram of unamplified image.

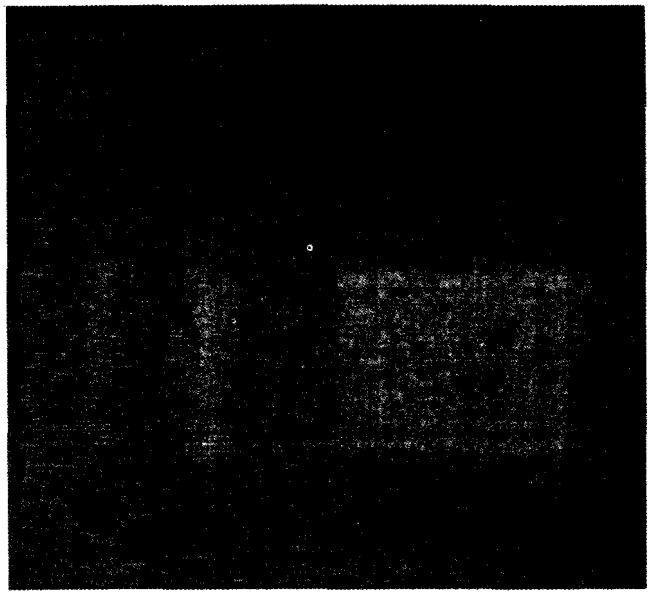

Fig. 6a: Amplified image A

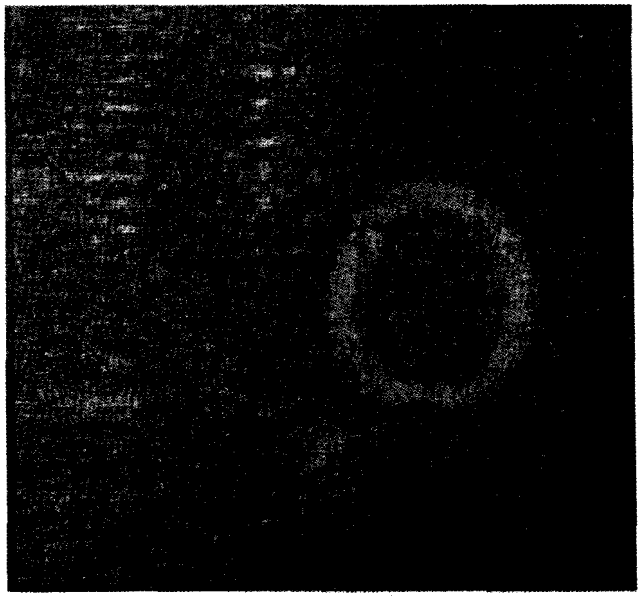

Fig. 6b: Amplified image B

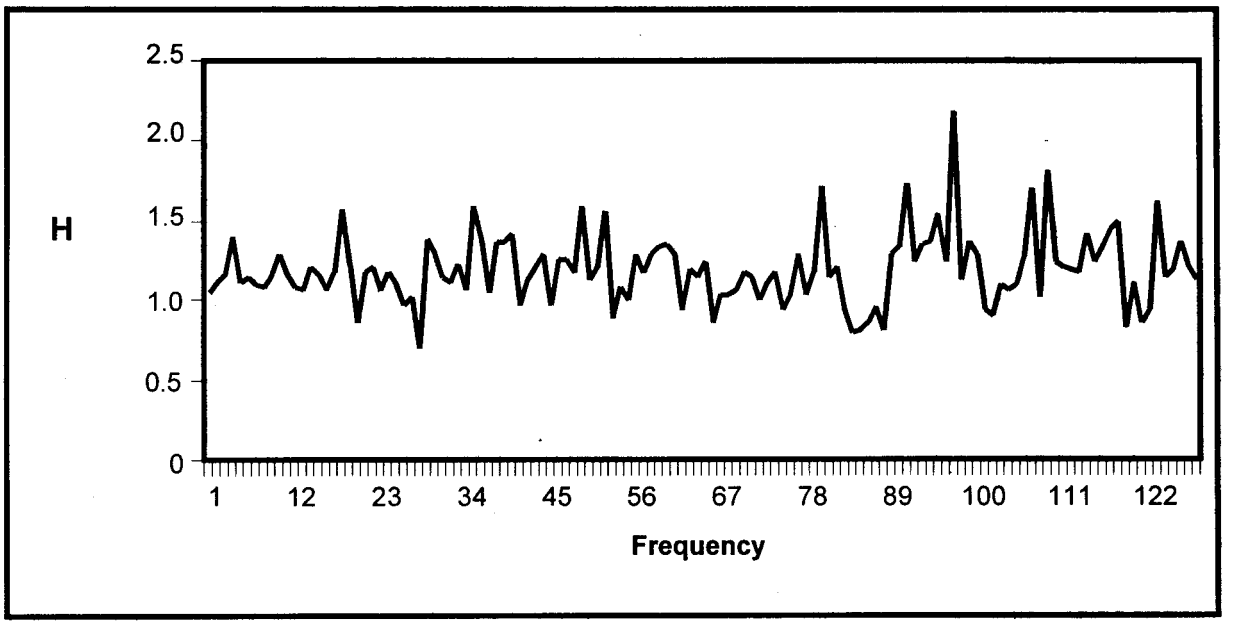

Fig. 7a. Response function Fourier transform along x-axis for Image A from low to high spatial frequencies.

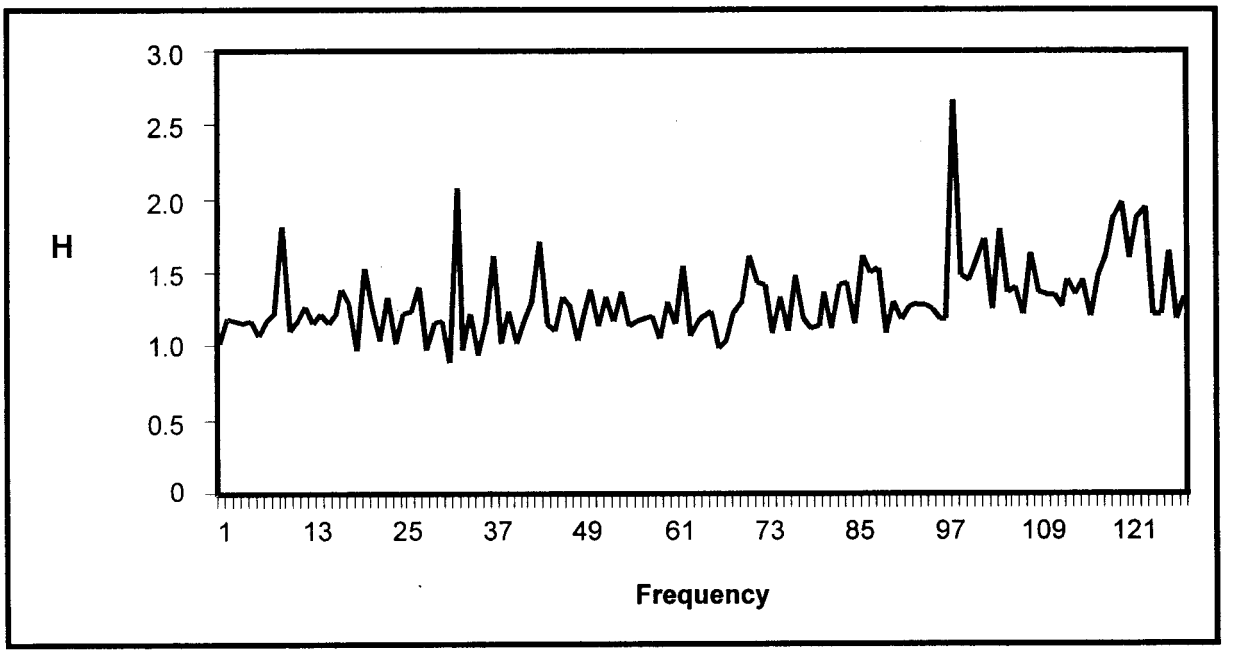

Fig. 7b. Response function Fourier transform along x-axis for Image B from low to high spatial frequencies.

Dividing the amplified FT by the unamplified FT will result in *H*, the Fourier transform of the response function. Its values may be related to the sensitivity of the system at a certain spatial frequency. In Fig. 7a , the response function FT along x for Image A has small fluctuations about 1 with a maximum value of 2.2. This peak occurs at pixel 99, which corresponds to a high frequency component. Also in this figure, the mean value of *H* for Image A is 1.2. Fig. 7b shows that Image B's x-axis response function FT peaks at pixel 100 (a high frequency component) with a value of 2.7. It also has small fluctuations about 1 with a mean of 1.3.

The response function FTs show sensitivity at higher spatial frequencies. Both have similar peaks and approximately the same behavior. *H* is essentially the same in both images.

CONCLUSION

Gray scale images were successfully amplified by TWM in a BSO crystal. The amplified images are observed to have higher gray levels, with an average relative gain of 5.9 compared to the original image. For the entire image, contrast range is enhanced from 0 to 58 to 0 to 98 and the overall brightness was increased by a factor of 2.7. The response function shows sensitivity at higher frequencies and is similar in two different images. Essentially, the set-up shows great potential as a coherent image amplifier and a possible component in an optical computing system.

REFERENCES

Joseph, J., P. K. C. Pillai, & K. Singh, 1995. Optical computing and image processing: the role of nonlinear photorefractive crystals, Proc. of the 2nd Winter College on Optics, Italy, 59-103.

Kawata, S., Y. Kawata, & S. Minami, 1990a. Image amplification with local addressing by two-wave coupling in a BSO crystal application of DC voltage. JOSA B 7(22): 2362-2368.

_____, 1990b. Locally controllable Image amplification by two-wave coupling with a BSO crystal, *Japanese Journal of Applied Physics* 29(8): L1547-L1549.

Tarroja-Keller, M. F., J. Natividad, D. Palima, R. Guerrero, & S. Baun, 1997. Amplification of light by a drift-type photorefractive crystals, Proc. of the 15th National Physics Congress, Cebu City, 31 pp.

Yeh, P., 1992. Photorefractive phase conjugators. Proc. of the IEEE, 80(3).

_____, 1993. Introduction to photorefractive nonlinear optics. New York: Wiley, 137 pp.